A Practical Guide to Using Boron Doped Diamond in Electrochemical Research

Journal:	*Physical Chemistry Chemical Physics*
Manuscript ID:	CP-PER-09-2014-004022
Article Type:	Perspective
Date Submitted by the Author:	08-Sep-2014
Complete List of Authors:	Macpherson, Julie; University of Warwick, Department of Chemistry

A Practical Guide to Using Boron Doped Diamond in Electrochemical Research

Julie V. Macpherson,* Department of Chemistry, University of Warwick, Coventry, CV4 7AL UK

Conducting, boron doped diamond (BDD), in addition to its superior material properties, offers several notable attributes to the electrochemist making it an intriguing material for electrochemical research. These include the widest solvent window of all electrode materials; low background and capacitive currents; reduced fouling compared to other electrodes and; the ability to withstand extreme potentials, corrosive and high temperature/pressure environments. However, BDD is not your typical electrode material, it is a semi-conductor doped degenerately with boron to present semi-metallic characteristics. Input from materials scientists, chemists and physicists has been required to aid understanding of how to work with this material from an electrochemical viewpoint and improve electrode quality. Importantly, depending on how the BDD has been grown and then subsequently treated, prior to electrochemical measurement, the resulting material properties can vary quite significantly from one electrode to the next. This likely explains the variability seen by different researchers working on the same experimental systems.

The aim of this "protocols" article is not to provide a state-of-the-art review of diamond electrochemistry, suitable references are provided to the interested reader, but instead serves as a reference point for any researcher wishing to commence work with diamond electrodes and interpret electrochemical data. It provides information on how best to characterise the material properties of the electrode before use and outlines the interplay between boron dopant density, non-diamond-carbon content, grain morphology, surface chemistry and redox couple identity. All should ideally be considered when interpretating electrochemical data arising from the diamond electrode. This will aid the reader in making meaningful

comparisons between data obtained by different researchers using different diamond electrodes. The guide also aims to help educate the researcher in choosing which form of BDD is best suited to their research application.

Submitted as a "Protocols" Perspective article to ***PCCP*** *j.macpherson@warwick.ac.uk

Introduction: Carbon electrodes have found wide-spread use in many different electrochemical applications e.g. sensing, fuel cell catalyst supports, with sp^2 carbon proving particularly popular *e.g.* glassy carbon (GC), highly ordered pyrolytic graphite, edge plan pyrolytic graphite, carbon nanotubes *etc*.[2] However, sp^3 carbon, *i.e.* diamond, is now finding significant use as an electrode in a variety of different application areas, which have been highlighted and reviewed in detail, for example in references 3,4,5,6,7,8,9. There is a wealth of data on diamond electrodes in the literature, however for both inner and outer sphere different redox couples, contrasting results can be reported. It is thus timely to consider the practicalities and peculiarities of using an sp^3 carbon material in electrochemical research, **especially** for the first time user.

Inner and Outer Sphere Redox Couples: Electrochemical redox couples fall generally into two categories, outer and inner sphere. For those that are outer sphere, electron transfer is often fast and the species comes close enough to the electrode for electrons to tunnel or hop across at least a monolayer of solvent. They do **not** directly interact with the surface and are often referred to as surface insensitive.[1] In contrast for inner sphere species there is a strong interaction between either the reactant or product with the surface, whereby reactants, intermediates or products are often specifically adsorbed. Inner sphere species are therefore considered surface sensitive.[1]

Diamond is an exceptional material, the complete sp^3 hybridisation of carbon results in extensive tetrahedral bonding throughout the lattice, leading to many extreme properties;[10] most notable are the hardness, very high thermal conductivity and extremely high electrical resistivity; diamond is a very wide band gap semiconductor (5.47 eV at 300 K).[10] The latter makes diamond, at first glance, useless to an electrochemist, unlike sp^2 materials in their intrinsic state. However, just as with silicon, where dopant impurities can be added to modify

electrical properties the same is true of diamond. Either side of carbon in the periodic table sits boron to the left (p-type dopant) and nitrogen to the right (n-type dopant). As boron effectively takes up the same position as displaced carbon atoms, with a relatively small activation energy (0.37 eV), unlike nitrogen (1.7 eV), high doping levels are possible. Thus boron is the preferred dopant for electrochemical studies.

In the literature, the regularly quoted favourable properties of boron doped diamond (BDD) electrodes include:[3,4,5,6,7,8,9] (i) wide solvent window; (ii) low background currents (low capacitance); (iii) reduced fouling; (iv) non-corroding at high temperatures, pressures and in challenging environments; and (v) biocompatibility. However, it is important to note the growth procedure adopted to synthesise BDD can affect the reported properties. Moreover, for the first time user, working with this material is not always as straight forward as with other conventional "metallic" electrode materials. In this protocols article, a guide to working with BDD electrodes and interpretating the data obtained is presented in terms of an understanding between the intimate relationship between material properties and electrochemical performance.

Growing BDD

Since the mid 1950's, it has been possible to synthetically produce diamond using high pressure high temperature (HPHT) methodologies.[11] Technological advances in the late 1980's resulted in the synthesis of diamond from gas phase carbon species using a chemical vapour deposition (CVD) technique at low pressures.[12] CVD growth of diamond relies on the generation of carbon radials and relatively high concentrations of disassociated hydrogen (H). High growth surface temperatures are also required, typically greater than 700°C, to provide the appropriate surface kinetics.

For commercial and laboratory electrode production CVD is by far the most popular growth technique, due to the efficiency of the process in controlling dopant incorporation and the ability to grow over large areas and on structured substrates. During CVD a plasma is created using either hot filaments (HF) or microwaves (MW). MWs enable the generation of higher plasma temperatures than HF, where temperatures are limited by the melting point of the filaments. The resultant higher temperatures of MW-CVD result in higher concentrations of H atoms. Most commercial BDD electrode manufacturers adopt the HF-CVD approach due to the ability to grow over large surface areas. However, with MW-CVD it is possible to achieve higher phase purity and faster growth.

A carbon source, such as methane, and dopant, boron, in gaseous form, e.g. B_2H_6, $B(OCH_3)_3$[13] *etc* is fed into the CVD reactor chamber, in the presence of hydrogen (H_2). H_2 is essential as the plasma generated H atoms terminate dangling surface bonds, prevent reconstruction of the surface and react with sp and sp^2 carbon sites, to preferentially etch them from the growth layer.[14] The employed growth parameters are hugely important as they will control properties such as the ratio of non-diamond-carbon (NDC) to diamond (qualitatively considered as an sp^2 to sp^3 ratio) the thickness of the film, texture and grain size.

The use of polycrystalline substrates results in polycrystalline diamond films, which contain diamond crystals of different growth facets, or grains. The growth substrate must be stable under the CVD growth conditions and have a low expansion coefficient. Suitable substrates include *e.g.* Si, Nb, Mb, Ti, Ta and W appropriately treated *e.g.* abrasion, seeding with diamond nanoparticles or electrical biased, to provide an increased density of nucleation sites for the promotion of diamond synthesis.[15] The resulting grain size depends on growth conditions such as time, temperature, pressure, gas composition e.g. hydrogen to carbon and boron ratios, the addition of noble gases such as argon *etc*.[16] This leads to the following

categories of BDD: (i) ultra-nanocrystalline (UCN), grain size < 10 nm;[15] (ii) nanocrystalline (NC), grain sizes in the range 10 nm – 1 μm[15] and; (iii) microcrystalline (MC), grain sizes > μm.[17] As crystallographic orientation affects boron uptake, with (111) > (110) > (100),[18] it is also important to consider that a polycrystalline surface will be heterogeneously doped.

NDC incorporation is thought to occur predominantly at grain boundaries, although incorporation into individual growth facets is also possible. Thus NDC can be electrochemically significant in UNC and NC BDD[15] given that the grain boundary density is significantly higher than in MC BDD. It is virtually impossible to grow UNC free of NDC. As dopant (boron) concentrations are increased it is also harder to prevent NDC formation, even in MC BDD. However, growth techniques have been perfected such that growth of highly doped MC BDD with negligible NDC is now possible.[19] For fixed growth conditions, as growth time increases, the size of crystalline facets increase with film thickness, as shown in Figure 1. Higher quality (lower NDC content) NC BDD films can be obtained using the growth conditions for MC BDD (high ratio of H atoms to methyl radicals) but stopping before the grains become too big.[15] UNC and NC films are therefore thin (tens of microns and smaller, especially for UNC) and for handling purposes are left attached to the growth substrate. MC films are much thicker and can be removed from the growth substrate. In this format they are often referred to as freestanding.

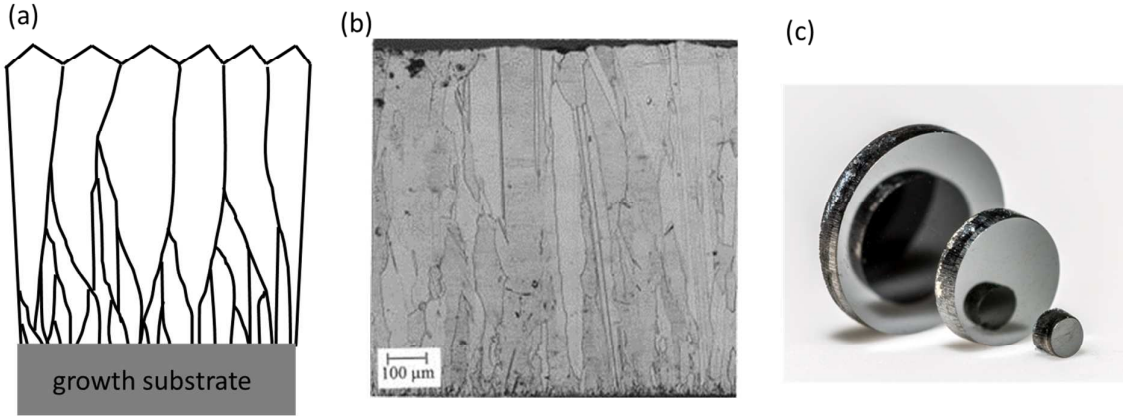

Figure 1: (a) Schematic and (b) scanning electron microscopy (SEM) image of the side on growth of MC BDD. Both clearly show how the grains increase with size as the film thickness increases. (c) Optical image of freestanding MC BDD (image copyright Jonathan C. Newland 2014) which has been removed from the growth wafer, lapped on both sides, and laser cut into discs.

For CVD of single crystal (sc) BDD, sc diamond itself is used as the growth substrate in order to encourage homo-epitaxial growth. These substrates are typically grown using HPHT technologies, where a synthesis capsule containing graphite and seed crystals are compressed to tens of thousands of atmospheres (~ 5 GPa) and heated to over 1800 K, in the presence of a metal solvent.[20] Although, this process has been used to synthesis industrial grade sc diamond for many years the diamonds produced are often small, in the micron to millimetre range, and are doped with nitrogen. For CVD scBDD synthesis, understanding the growth mechanism enables optimisation of the growth conditions[21] to produce electrodes with minimal defect density and impurity incorporation.[22] However, maturity in the field of scBDD is nowhere near as advanced as for polycrystalline BDD, as reflected in the number of research papers produced using the two different classes of materials. As of yet there are no commercially available sc BDD electrodes.

Material Properties of BDD

In the laboratory researchers can obtain BDD electrodes from three different sources: (1) from their own home-built systems; (2) from commercial growth systems e.g. MW plasma CVD reactors from e.g. Seki Diamond Systems, Microwave Enterprises, Diamond Materials and iPlas Cyrannus or; (iii) purchase from a commercial company, as listed in Table 1. Regardless of the source, the following are important considerations which must be taken into account when interpreting the resulting electrochemical behaviour.

1. Surface morphology
2. Amount of boron in the material
3. Surface termination

4. Presence of NDC
5. Surface finish

1. Surface Morphology: Visualisation of the surface is best achieved using SEM and will help identify the category of polycrystalline BDD employed *e.g.* UNC, NC or MC, as shown in Figure 2. Techniques such as atomic force microscopy (AFM) or interferometry are often employed in conjunction with SEM in order to accurately determine grain size and define surface roughness, which is important when determining the double layer capacitance, C_{dl}, of the material.

For MC BDD electrodes, especially those that have been polished, contrast in the SEM image can be used to qualitatively inform on differences in dopant levels across the surface.[23] Note, using SEM can NDC contaminate the surface hence the electrode must be cleaned after imaging. In general, for a stringent clean, boiling concentrated H_2SO_4 (98%) acid supersaturated with KNO_3 is recommended.[24] This procedure works well for freestanding, thick BDD, but can be too aggressive for thin BDD films still attached to the growth substrate, as it can etch the substrate, causing the diamond to separate from its support. For these materials, electrochemical treatment in a lower concentration acid is preferred.[25,26]

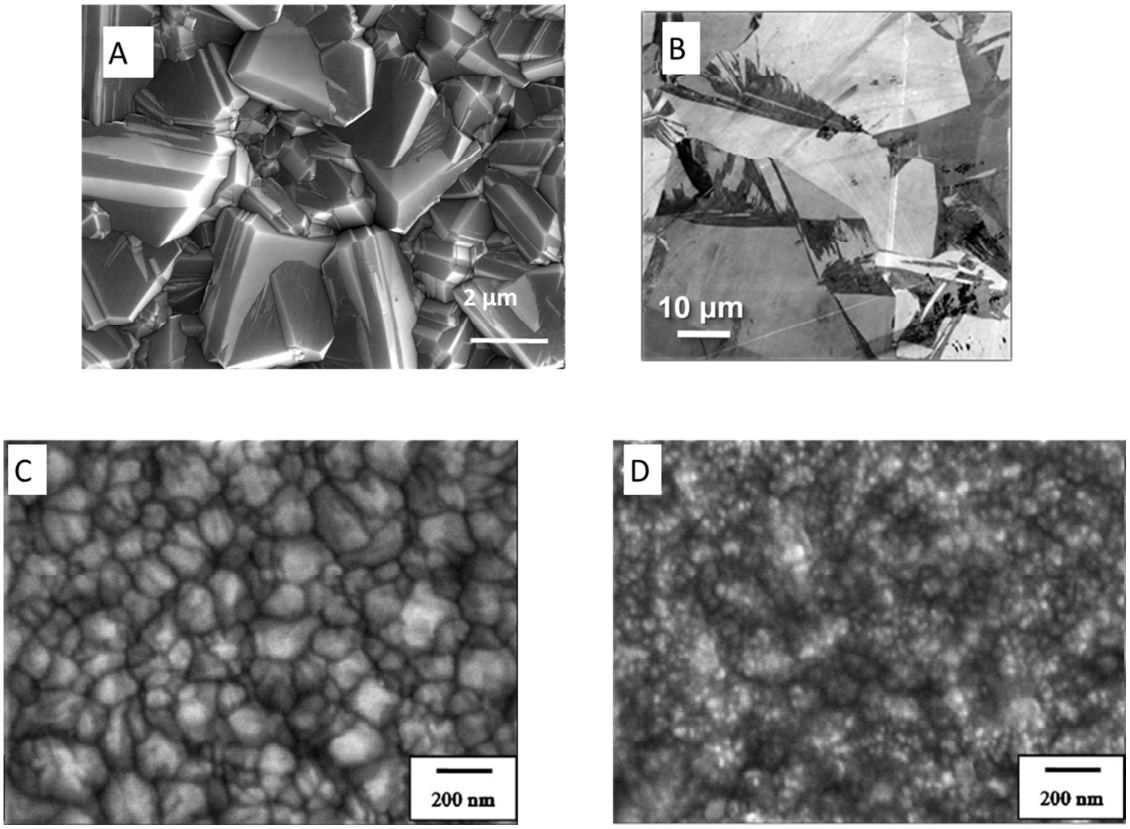

Figure 2: (a) SEM of as-grown MC BDD; (b) SEM of a polished "lapped" surface of MC BDD. Zones of darker intensity correspond to more heavily boron doped regions of the surface. Taken from reference [27] with permission. (c) SEM of BDD NC thin film and (d) SEM of BDD UNC thin film. Both (c,d) taken from reference [28] with permission.

2. Boron dopant density: BDD is not a conventional electrode material. Diamond by definition is a very wide band gap semiconductor, containing ~ 2×10^{23} C atoms per cm^3 in the diamond lattice. Doping with boron introduces p type acceptors (holes) into the lattice. Doping with enough boron such that the acceptor density is so high there is significant wave function overlap of acceptor atoms, enables hole propagation without thermal activation to the valence band.[29] The material can now be described as semi-metallic or "metal-like" but with a reduced number of charge carriers or density of states (DOS),[27] compared to a classical metal.

As a rule of thumb, typically ~ 2 in 1000 C atoms must be replaced by B in order to demonstrate degenerate doping and semi-metallic properties, *i.e.* dopant densities greater than ~ 10^{20} B atoms cm^{-3}. For dopant densities less than this the material will show hopping transport characteristics and then p-type semi-conducting properties at dopant densities of ca. 10^{19} B atoms cm^{-3} and lower. Charge carrier availability for electrochemistry decreases as the dopant density decreases.[30] This is accentuated at applied electrode potentials less positive of the flat band potential (E_{FB}) of semi-conducting BDD. E_{FB} refers to the applied potential where there is no band bending or charge depletion.[31] Hence it is essential to know the boron dopant density of the material you are working with. Qualitatively, colour gives a good indication with black diamond suggesting high "metallic" boron content. Although as a note of caution, when insulating diamond has been grown with a high NDC content, arising from small grains and fast growth, it too can look black. Blue diamond is qualitatively indicative of semi-conducting BDD.

The boron concentration is typically expressed in three ways, either in (i) ppm, which relates to the concentration of boron in the gas phase with respect to the carbon source; (ii) % of boron to carbon in the gas phase or (ii) number of boron atoms per cm^3 in the solid phase. (i) and (ii) provide qualitative indications as to whether the diamond contains enough boron to be considered metal-like, but are not quantitative. To obtain a quantitative value expressed in boron atoms per cm^3 it is necessary to use techniques such as secondary ion mass spectrometry (SIMS, used by the majority) or boron nuclear reaction analysis. It is important to also consider how the boron content measurement area compares to electrode grain size.

As shown in Figure 3, the resistivity, ρ, of BDD relates to the boron dopant density.[30] For comparison with the data in Figure 3, Pt and Au have ρ values of 1.06×10^{-5} Ω cm and 2.2×10^{-6} Ω cm (at 20 ^{o}C), respectively.[32] ρ is typically measured using a four point probe approach. It is also possible to make temperature dependant resistivity measurements, which

inform more precisely on the electrical transport mechanism e.g. metallic, hopping, valence band conduction. However, as ρ measurements do not discriminate between BDD and NDC, NDC presence may decrease the measured ρ values resulting in an assumption of a higher boron concentration than actually present.

For semi-conducting BDD, Mott Schottky plots recorded in electrolyte solutions, enable determination of both E_{FB} and the number of uncompensated charge carriers.[33,34,9] A reduction in the number of freely available charge carriers for ET in BDD is possible via *e.g.* compensation of boron acceptors with suitable donors, such as nitrogen[35] and charge trapping due to the presence of defects and impurities in the diamond lattice.[36] This means the boron dopant density measured using techniques such as SIMS may not accurately reflect the actual number of charge carriers available for ET. This is especially true for lower doped BDD electrodes with a high impurity/defect concentration.

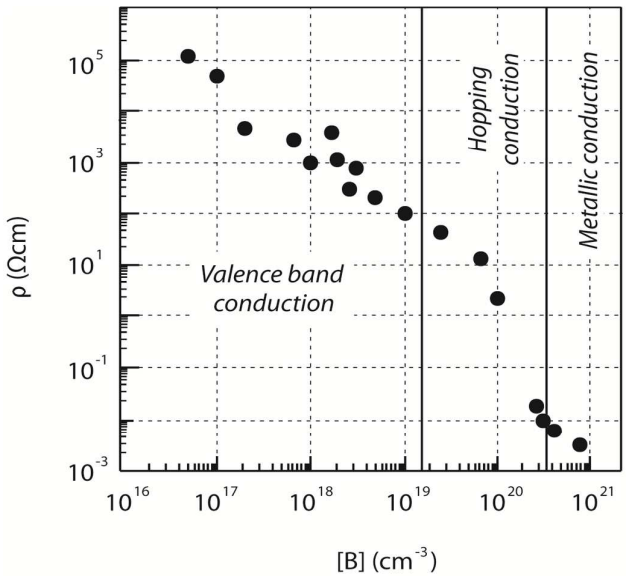

Figure 3: Room-temperature resistivity as a function of boron doping concentration (taken with permission from [30]).

3. Surface termination: Understanding the surface termination of a BDD electrode is important for several reasons: (1) electrode surface functionalisation can strongly influence the electron transfer (ET) kinetics of inner sphere redox processes.[1] (2) BDD surface

termination affects the wetting properties of the electrode. (3) The polarity of the surface bond results in electrostatic interactions which can raise or lower the energy levels of the valence (E_{VB}) and conduction bands (E_{CB}). For example, hydrogen (H-) terminating the diamond surface ($-C^{\delta-} - H^{\delta+}$) results in a raising of both E_{VB} and E_{CB}, with the latter sitting above the vacuum level; negative electron affinity. This results in an interesting phenomenon when the diamond is immersed in solution which must be considered when interpreting electrochemical responses. Specifically, ET between the E_{VB} and $H_3O^+_{(aq)}$ becomes possible and a positively charged accumulation layer, sub-surface is formed. This surface transfer doping[37,38,39,40] process results in a measurable surface conductivity.

Diamond grown in a CVD plasma reactor leaves the growth chamber H-terminated, provided an appropriate cool-down under a hydrogen atmosphere is implemented. This results in a hydrophobic surface displaying water contact angles as high as ~ 90^o (insulating diamond), Figure 4.[41] Interestingly, there is evidence that as BDD content is increased the hydrophobic contact angle decreases.[34] A H-terminated surface is often stable in air for several months, however it will slowly oxidize with time,[42,43] becoming more hydrophilic. Surface oxidation is also possible by electrochemical means, typically by anodically polarizing.[19] O-terminated surfaces $''C^{\delta+} - O^{\delta-}''$ have an opposite bond polarity to H-terminated ones which typically results in lowering of the energy levels and a positive electron affinity.

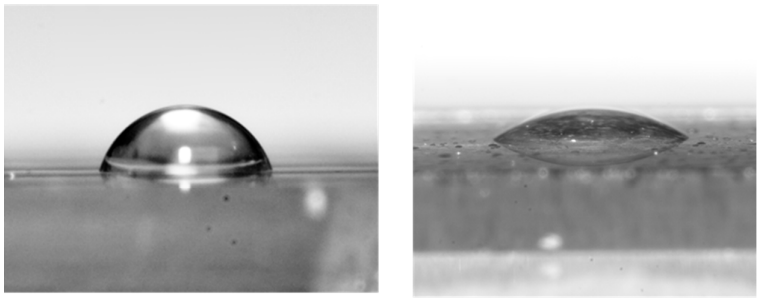

H-terminated O-terminated

Figure 4: Contact angle measurements taken on H-terminated and O-terminated boron doped diamond surfaces.

It is important to periodically check surface termination to ascertain what the surface state is, especially if a H-terminated electrode has been used extensively in the anodic window during cyclic voltammetric (CV) or chronoamperometric analysis.[19] This can be done most simply by running contact angles, as shown in Figure 4. An oxidized surface surface results in water contact angles ranging from 0.6^{o} to 65^{o} depending on the method of O-termination, surface roughness *etc*.[44] To deliberately convert from H-termination to O-termination a variety of different techniques have been employed[9] including boiling in acid,[45] alumina polishing,[19] exposure to oxygen plasma,[28,46] photochemical oxidation,[41] reaction with oxygen at high temperatures,[47] and as highlighted above anodic polarisation.[48,46, 49,26]

For more precise chemical information on surface functionalization, measurement techniques such as X-ray photoelectron spectroscopy (XPS) are required.[28,49] Different oxidation procedures will result in different chemical functionalities; a phenomenon also controlled by the proportion of different grain orientations on the polycrystalline electrode surface. For example, studies on oxygen-terminated single crystal diamond showed that C-OH groups are most abundant on the (111) face. However, C-O-C and >C=O (and more highly oxidised) groups dominate on the (100) face, with the method of treatment determining the ratio of different groups on the surface.[50] Surface chemistry, in turn, will strongly affect the electrochemical ET characteristics of inner sphere species. Thus for the interpretation of ET kinetics, it is important to know which chemical groups are on the surface and how stable they are in the potential window of interest when carrying out the electrochemical reaction.

For samples bought commercially it is also important to check the surface termination before use, again most simply by using contact angles. Even samples which start life H-terminated, dependant on the length of time on the shelf or the processing procedures

employed to package the electrode, may no longer be fully H-terminated. There has been discussion in the literature as to whether cathodic polarisation of the electrode can re-hydrogenate the surface.[43,51,52] Applying a negative voltage in acidic solutions (typically ~ -3V versus Ag/AgCl in 0.5 M H_2SO_4) to generate hydrogen has been proposed as a means of H-terminating the surface. However, as no direct comparisons have been made between the quality of the resulting surface after electrochemical treatment and that from hydrogen plasma, it has been questioned whether these procedures actually replicate the as-grown H-terminated surface.[53] Interestingly, many papers in the literature will simply refer to a cathodically treated BDD as H-terminated. Severe cathodic potential treatment, -35 V for 5 mins in a 2 M hydrochloric acid solution, has also been advocated as a means of producing a H-terminated surface more akin to that produced by the H-plasma process.[53] However, to-date, it is still widely believed the only reliable way to reconvert the surface back to its fully H-terminated state is exposure to hydrogen plasma or to hydrogen dose.[40]

4. NDC presence: The more NDC present in the BDD matrix, the less electrocatalytically inert the electrode is. Electrochemically, this typically means a reduced solvent window, increased background and capacitative currents[19,54] (and decreased limits of detection) and a surface potentially more susceptible to fouling.[55] NDC presence can also change the way the electrode behaves towards different redox systems, especially those that are surface sensitive. Hence it is important to know whether the electrode contains NDC and if so, how it impacts your measurement of interest. For example, in one study it was shown electrodes with increasingly higher levels of sp^2 favoured electrochemical conversion, rather than combustion, of a model pollutant,[56] whilst others have shown increasing sp^2 results in more facile ET kinetics for certain inner sphere redox couples.[54] The easiest way to qualitatively check for NDC is using Raman microscopy; this technique is also able to provide a qualitative assessment of boron content.

Raman microscopy: Pure diamond contains only sp^3 carbon (σ bonds) which in a Raman spectra results in a single diamond zone centre optical phonon peak (referred to herein as the sp^3 peak) occurring at 1332 cm^{-1}. The line width is a qualitative measure of the crystalline quality of the film. The more defects, the shorter the phonon lifetime and the broader the line width. NDC (sp^2 containing diamond - π bonds) in the matrix produces two peaks, G and D. The G peak is a result of stretching of pairs of sp^2 sites (rings and chains) whilst the D peak is the breathing mode of sp^2 rings. In crystalline graphite the G peak occurs at 1575 cm^{-1}, whilst the disordered D peak occurs at 1355 cm^{-1}. For amorphous carbon, the peak widths of the D and G peaks are generally broader, depending on the ordering of the NDC material.

NDC π bonds are more polarisable than sp^3 σ bonds, and have a larger Raman cross section, for example at 514.5 nm excitation the Raman scattering is ~×50 more sensitive to π bonded graphite and amorphous carbon, than diamond.[57] In general as the excitation wavelength increases the scattering becomes more sensitive to sp^2 and less sensitive to sp^3 carbon. In Raman, selection of the correct laser wavelength is thus important to accentuate the features of interest, therefore quoting the Raman wavelength when stating the observed sp^3/sp^2 ratio is also important. Popular laser choices in Raman include 514.5 nm green Ar ion laser, 632 nm visible HeNe laser and 785 nm IR diode laser. The relative intensity of the sp^3 peak to the sp^2 G peak, as seen in Figure 5(a) is often used as a qualitative assessment of the quality of the diamond material. However, as resolution (depending on optical magnification) tends to be of the order of microns, it is important to make many measurements across the sample, especially when the diamond grain size is bigger than the laser spot size.

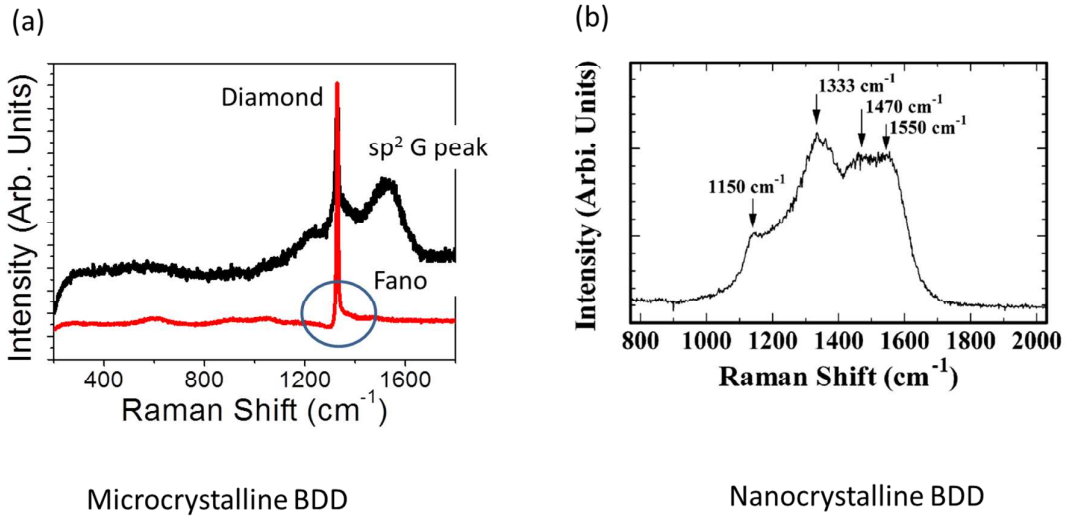

Figure 5: (a) Visible Raman spectrum for a lapped MC BDD electrode at laser wavelength = 514 nm and power = 10 mW. The red line is taken in a lower doped region of the surface which shows no evidence of sp^2 carbon. The asymmetry "Fano resonance" of the diamond peak indicates "metallic" doping. The black line is taken in a higher doped region, where sp^2 carbon is now evident. Taken from reference [19] with permission. (b) Visible Raman spectrum for a NC BDD thin film electrode at laser wavelength = 532 nm and power = 50 mW. Integration time = 5 s. Taken from reference [58] with permission.

As the boron concentration increases the diamond sp^3 peak shifts to slightly lower wavenumbers[59] and moves from being symmetrical to deforming asymmetrically, typically observed for boron concentrations ~ ≥ 10^{20} B atoms cm^{-3}, as shown in Figure 5(a). This feature is attributed to a Fano-type interference between the discrete zone centre optical phonon and a continuum of electronic excitations,[60] and signifies the onset of metallic conductivity on the boron impurity band.[61] Hence observation of a Fano resonance is further proof the diamond has been doped with sufficient boron to be deemed "semi-metallic".

As the boron doping levels increase the intensity of the diamond peak (and area under the peak) decreases and the peak becomes more asymmetric. Analysis of peak intensity (or area) is also another way to qualitatively map boron doping levels in the electrode.[23] This measurement is best suited to larger grained MC electrodes where the spot size of the laser can interrogate individual grains. Broad features at ca. 500 cm^{-1} and 1220 cm^{-1} have also been

observed for highly doped BDD in the range 10^{20} – 10^{22} atoms cm^{-3} [60]. Features in the range 1350-1580 cm^{-1} are often associated with NDC.

As the crystallite size is decreased the material becomes more disordered and the Raman spectra becomes more complicated to interpret as selection rules break down. For NC and UNC BDD this results in the shifting, broadening and asymmetry of existing peaks and even the occurrence of new ones, as seen in Figure 5(b).[58] The sp^3 peak broadens and overlaps with the D band associated with NDC present in grain boundaries.[15] A characteristic peak at 1150 cm^{-1} is also often observed thought to originate from sp^2 hybridised structures present on the surface and at grain boundaries, such as polyacetylene type molecules.[62,63,64]

5. Surface finish: BDD electrodes are often found in two states, as-grown and polished. The surface can also be chemically etched before use. For the as-grown surface, MC BDD is inherently rougher than NC and UNC BDD, which must be taken into account when quoting capacitance values for the electrode. Microscopic visualisation of modified BDD electrodes, using scanned probe techniques, is also much easier the flatter the surface. Thin film electrodes, i.e. less than ~ 50 μm thick, tend to be left as-grown on the growth substrate, as polishing is difficult, and for NC and UNC electrodes is often unnecessary as surface roughness is << 1 μm. Thicker films are more amenable to polishing. Growing thick BDD (e.g. hundreds of μm's) results in large grain sizes and also means the material is mechanically robust enough to be removed from the underlying support material, as shown in Figure 1(c). The use of freestanding electrodes also means delamination from the underlying growth substrate when operating under certain electrochemical conditions[65] is never an issue.

Polishing requires specialised diamond impregnated polishing wheels and know-how in order to produce ~ nm scale roughness. In polycrystalline materials this process is referred to as lapping. Unless you are accomplished in the art of diamond polishing this is to be avoided as a poorly controlled polishing process will result in sub-surface damage creating

defects which trap charge carriers. For highly doped "metallic" MC BDD it has been shown polishing using a carefully controlled process has a negligible effect on the electrochemical characteristics of the electrode.[19]

ELECTROCHEMICAL MEASUREMENTS:

Once the key material properties of the electrode have been characterised as described above, the electrode is then ready for deployment in an electrochemical cell. The following require consideration before use in the application area of interest.

1. Electrical contact to the BDD electrode
2. The electrochemical cell arrangement
3. Solvent window and capacitance quantification
4. Assessment with outer sphere redox mediators

1. Electrical Connection: Once the material has been synthesised in house or purchased, it is necessary to make an ohmic electrical connection. A poor contact leads to contact resistance, which results in ohmic drop effects in voltammetric measurements. Unlike nearly all other electrode materials a good ohmic contact to the diamond surface cannot be made by simply using silver paste or solder as most metals on (O-terminated) diamond result in a Schottky contact.[66] The trick is to form an ohmic metal carbide contact with the BDD surface. This can be achieved using metals such as Ti, Cr, Mo[67,68] although the most common approach is to sputter a thin layer of Ti onto the BDD surface, followed by an inert metal, such as Au or Pt. Critical to the process is an annealing step which results in the formation of the ohmic titanium carbide contact. For thin film material still on the growth substrate, a top contact can be made this way or in the case of doped silicon (or Nb) substrates, a bottom electrical contact can be made directly to the conducting substrate.[9, 25,69]

Note, for making electrical contact to H-terminated BDD with Ti/Au comes with problems. The annealing temperature required to make a carbide contact is likely to destroy the H-termination layer. If the only means of connecting the electrode is direct contact to the BDD surface then the use of silver paint can be considered. H-termination of the BDD electrode results in band bending and a better alignment of energy levels between the H-terminated BDD electrode and *e.g.* Ag or Au.[66] However, it is important to measure the potential dependant contact resistance under these conditions to ascertain impact on the electrochemical measurement. If the user wishes to put down thin film Au as the contact, evaporation is preferred over sputtering; the harsher conditions of the sputtering experiment will typically destroy the H-termination layer.

2. Electrode configuration: Of importance to an electrochemist is how to work with an electrode so it can be used for the widest range of experiments imaginable. Conventionally, in the laboratory, electrodes are packaged such that they can be handled efficiently, are easily cleaned, and are of a known geometry. For some requirements, different electrode geometries and/or multiple electrodes in an addressable format are needed. Typical electrodes such as Pt, Au, and GC are available from a range of commercial suppliers, in macrodisk form, sealed in solvent resistant insulating plastics such as Kel-F or PTFE. Microdisk electrodes are also available and are often sealed in glass.

For BDD, electrodes in the recognised format, akin to Pt, Au and GC, are not currently widely available, hence alternative formats are typically adopted. For BDD on the growth substrate, an insulating cell *e.g.* Teflon, produced in house, is typically clamped on the top BDD surface with an O-ring in place to provide a water tight seal, as shown in Figure 6(a). Alternatively, PDMS mounts or insulating adhesives can be painted or adhered (e.g. Kapton tape, insulating epoxy) onto the electrode to define the electrode area. Using these

procedures, interrogation of a freshly H-terminated BDD surface is possible, as the electrode has not been subject to any mechanical or chemical treatment of the surface during electrochemical cell construction.

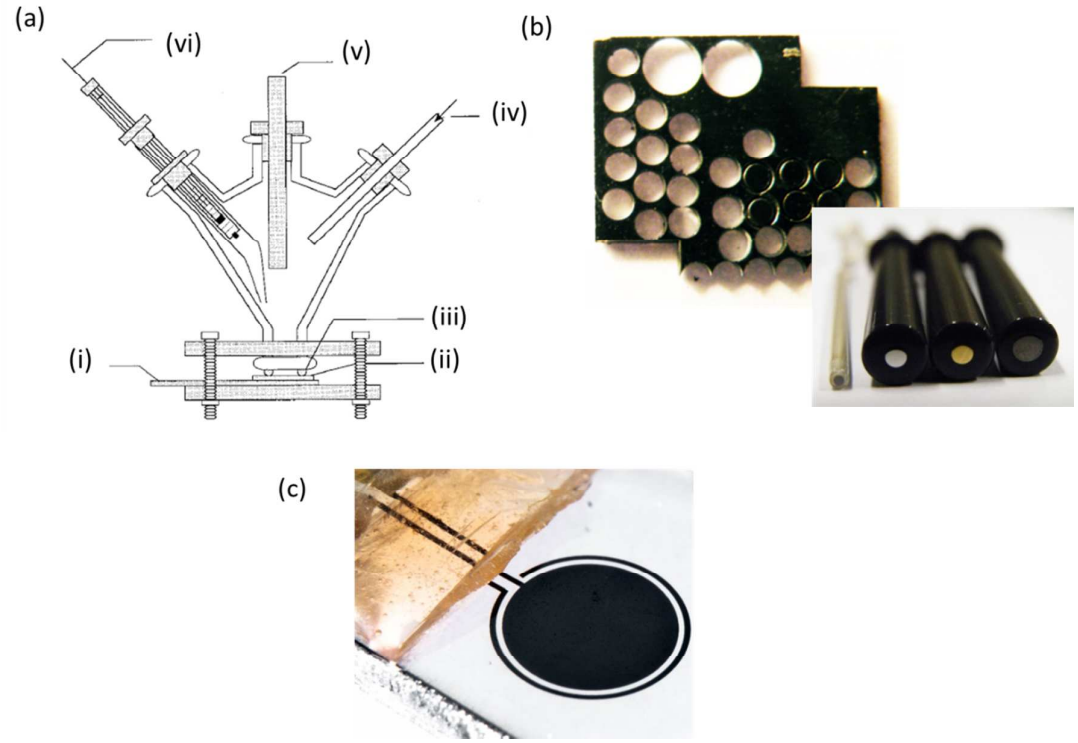

Figure 6: Different experimental arrangements used by researchers when working with BDD electrodes. (a) For thin film BDD still attached to the growth substrate a glass electrochemical cell can be used, adapted from reference [25] where (i) is a Cu or Al metal current collecting plate; (ii) is the diamond film electrode; (iii) is the Viton O-ring seal; (iv) the input for nitrogen purge gas; (v) carbon rod or Pt counter electrode and (vi) reference electrode. (b) Preparation of BDD freestanding electrodes, adapted from reference [24] with permission. A laser machiner is used to cut the required BDD electrode geometry from a BDD freestanding wafer. The electrode is ohmically contacted, sealed in glass and polished flat to reveal the BDD electrode to the left of the bottom left image. Also shown are conventional polymer sealed Pt, Au and glassy carbon electrodes. (c) Top contacted co-planar BDD ring disk electrode, sealed in diamond. The diameter of the disc electrode is 3 mm. Adapted from reference [70] and Jonathan Newland, copyright with permission.

For freestanding BDD, it is also possible to use a laser micromachiner to drill out a cylinder (or any geometry) of a defined diameter (Figure 6(b)) and then seal in epoxy or in a glass capillary using procedures adopted typically for sealing conducting microwires to

produce microelectrodes.[24] Note the laser cutting process can leave NDC around the cut edges, so the material must be stringently acid cleaned to try and remove as much NDC as possible before sealing. The entire front face is then mechanically polished to reveal the electrode material. As the BDD will always polish at a vastly slower rate than the surrounding insulator it is also important not to overpolish in order to avoid the BDD significantly protruding from its surroundings resulting in a non-coplanar arrangement.

If the user has access to lithographic processing equipment, there are also many procedures in the literature which describe the fabrication of well-defined "recessed" micro- and nano-array BDD electrodes, insulated with either diamond or silicon oxide.[71,72,73] Procedures also now exist for the formation of co-planar BDD electrodes (of any geometry) insulated with diamond[70] (Figure 6(c)), an approach which requires someone skilled in the art of diamond polishing to produce the final structure. However, working with diamond insulated BDD electrodes does have the advantage that the insulating material won't degrade when operating in extreme environments.

CVD enables BDD growth on structured surfaces this means that BDD electrodes in a non-planar format are also available. For example, microelectrodes can be produced by growing BDD on sharpened metal (*e.g.* W) wires.[74,75,76] Both NC- and MC-films can be formed, with the MC films showing less NDC content but a rougher surface, as expected.[75] The wires are typically seeded with diamond nanoparticles prior to growth. The challenge with BDD coated wires as with any metal wire is how to reliably insulate the wire such that only a defined (micro) portion of the tip is exposed and there are no pinholes in the insulating film. This problem is exacerbated the rougher the BDD film. A variety of different insulating films have been employed such as glass, epoxy, polyimide, nail polish, polypropylene tubing and electrophoretic paint, however, to-date the problem has still not been reliably solved.

3. Solvent windows: The solvent window defines the potential range over which an electrode can operate before the solvent is electrolysed. For a BDD electrode doped above the metallic threshold, and verified by Raman to contain negligible levels of NDC (sp^2) the solvent window in aqueous solution should demonstrate the following features, as shown by the black line in Figure 7(a). (i) A very extended potential window, compared to more conventional electrode materials such as Pt, Au and even GC. Please note the size of the window will be pH dependant, so it is important to quote the electrolyte (and concentration), pH and the current values (and scan rate) used to define the window. To enable comparison between different electrode geometries it is more useful to quote a geometric current density, as shown in Figure 7. Values in the literature range from 0.4 mA cm^{-2} [19] – 0.5 mA cm^{-2},[25] although very often it is not clear how the size of the solvent window has been defined. Typical solutions employed by researchers in the field to make solvent window measurements include *e.g.* (i) 0.1 M KNO_3;[19] (ii) 0.1 M/0.5M H_2SO_4;[25] (iii) 0.1 M $HClO_4$.[77] It is also useful to note the surface termination of the electrode as there are reports of the solvent window being narrower for H-terminated surfaces compared to O-terminated ones.[78]

(ii) For an NDC free BDD electrode, there should be no evidence of an oxygen reduction (ORR) signature in the CV under neutral and acidic conditions (Figure 7(a); black line). On Pt, ORR under alkaline conditions is thought to be outer sphere,[79] whether the same is true of BDD is currently under investigation. (iii) In the anodic potential range close to the solvent window there should be an absence of features associated with sp^2 carbon surface driven electrochemical features.

The reasons for the observations are described: (i) The sp^3 surface of BDD can be described as "catalytically inert." For efficient ET, water electrolysis requires the presence of catalytic sites on the electrode surface (inner sphere ET).[80] On BDD electrodes there are a lack of "binding sites" to mediate electron transfer between the surface and a water molecule.

Contrast this with Pt and GC, where both unfilled d orbitals (Pt) and reactive quinine-like groups (GC), respectively, enable more efficient water-electrode interactions (Figure 7(b)). Water electrolysis is thus more facile on these electrodes and the solvent window is reduced. (ii) Oxygen reduction (ORR) is also an electrocatalytic "inner sphere" ET process and requires interaction between the molecule and the surface for efficient ET (pH dependant). On BDD there are no suitable binding sites for oxygen, and thus oxygen reduction cannot take place at the electrode surface. When NDC (sp^2) is present, binding sites are now available and ORR becomes possible (Figure 7(a), purple line), although the process is not as facile as on *e.g.* Pt, which is an efficient electrocatalyst for oxygen (Figure 7(b)). ORR is observed on GC (Figure 7(b)) and graphite electrodes, but again the process is kinetically hindered compared to the noble metals. (iii) On NDC, hydroquinone/benzoquinone-like ET processes, associated with sp^2 carbon,[81,54] can take place at positive oxidising potentials (Figure 7(a), purple line). These are surface bound redox processes. Note, it is possible that if the surface is H-terminated, features (ii) and (iii) associated with NDC content can be (partially) masked.

If the surface does contain significant NDC, various reports exist to reduce sp^2 content. For example, it has been reported that acid washing followed by rehydrogenation of the surface or anodic polarization by cycling in acid solutions, can result in a reduction of sp^2 content.[25,26] It has also been noted that a similar effect can be achieved by employing a slow cool-down procedure in atomic H, post growth.[82] Examination of the CV response pre- and post-treatment is useful in assessing the effectiveness of the treatment process employed. More sophisticated approaches have adopted *in-situ* electrochemical Raman, to follow the sp^2 signature in response to an electrochemical cleaning procedure.[83]

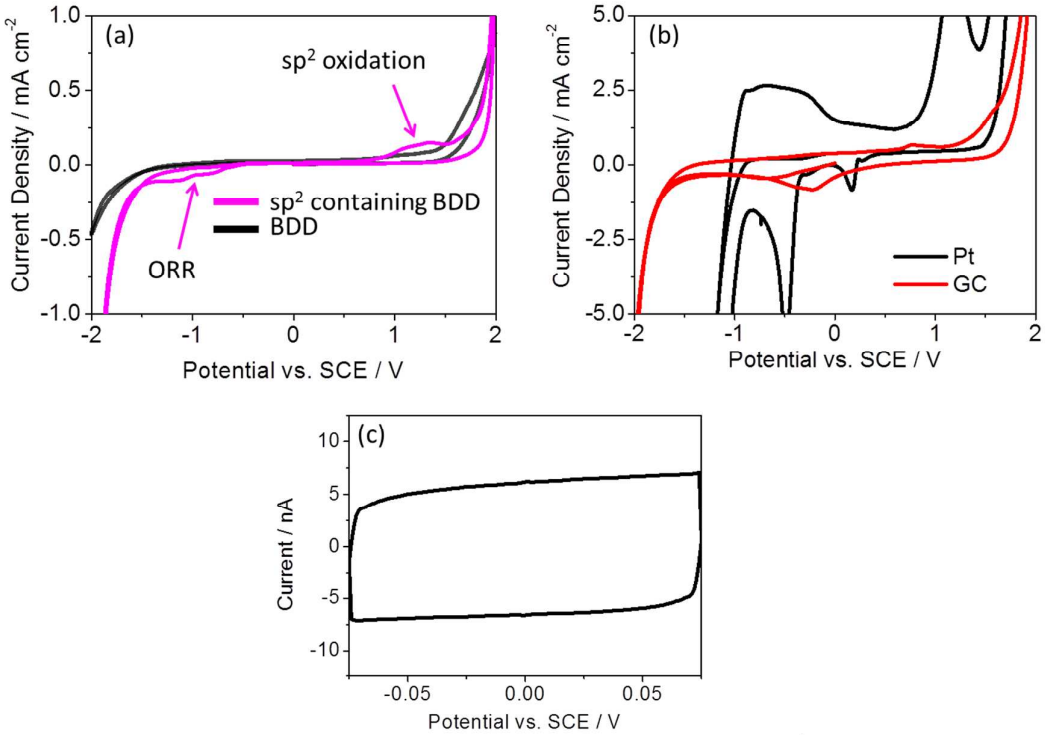

Figure 7: (a) Solvent windows recorded in 0.1 M KNO_3 at 0.1 V $s^{-1}$for: (a) freestanding MC BDD containing NDC (purple line) and negligible NDC (black line) and; (b) Pt (black line) and GC (red line). Adapted from reference [19] with permission. The current density have been plotted on a scale suitable to enhance the background currents. Note the scale in (b) is ×5 that in (a) and emphasises the low background currents obtained with BDD electrodes. (c) Typical capacitance curve recorded to enable calculation of C using equation (1). The CV was recorded in 0.1 M KNO_3 at 0.1 V s^{-1} over the potential range -0.1 V to + 0.1 V at a sp^2 free MC BDD electrode. Adpated from reference [19] with permission.

In the solvent window, high quality BDD passes very low currents, attributed to the low capacitance of the material (<< 10 μF cm^{-2}) compared to conventional electrode materials such as Pt and Au (~ 30 μF cm^{-2}).[84] This is a major reason for why BDD electrodes enable lower detection limits for trace analysis compared to other electrode materials. The low currents originate from three factors: (1) the lower DOS for BDD[27] compared to classical electrode materials. Increasing boron typically increases the measured capacitance, most likely due to an increasing DOS.[19] (2) The chemical stability of the sp^3 diamond surface. (3) A significant reduction in surface driven ET processes, especially when the BDD contains negligible levels of NDC.

Measuring C_{dl} of the material is a useful indicator of material quality. C_{dl} can be determined using equation (1) in conjunction with cyclic voltammetric (CV) measurements:

$$C = i_{av} / vA \qquad (1)$$

where i_{av} is the average current from the forward and reverse sweep, v is the scan rate and A is the electrode area. It can be difficult to accurately measure the electrode area as the surface becomes rougher e.g. for as-grown MC materials. Note, it is also possible to determine C_{dl} from electrochemical impedance spectroscopy (EIS) measurements.

4. Electrochemical response:

Of huge importance in electrochemical measurements is to make sure the boron dopant density (and more importantly free carrier concentration) is actually high enough for the electrode to behave "metal-like". The electrochemical applications for conducting diamond electrodes *i.e.* electrodes which are electrochemically active over a wide potential range far outweigh those for semiconducting electrodes, which are active only in a restricted potential window.

One simple electrochemical approach to assessing the suitability of the material is to record CVs using fast ET outer sphere redox couples that have a formal potential (E_o') lying in the band gap of semi-conducting O-terminated BDD (Figure 8). E_o' relates to the easy to measure, half wave potential, $E_{1/2}$ via:[85]

$$E_{1/2} = \frac{E_{p,a} + E_{p,c}}{2} = E_o' + \frac{RT}{2nF} \ln \frac{D_{red}}{D_{ox}} \qquad (2)$$

where $E_{p,a}$ and $E_{p,c}$ are the peak potentials for the anodic and cathodic components of the CV. R is the ideal gas constant, T is the temperature, n is the number of electrons transferred per redox event, F is Faradays constant and D is the diffusion coefficient of the two forms of the redox couple.

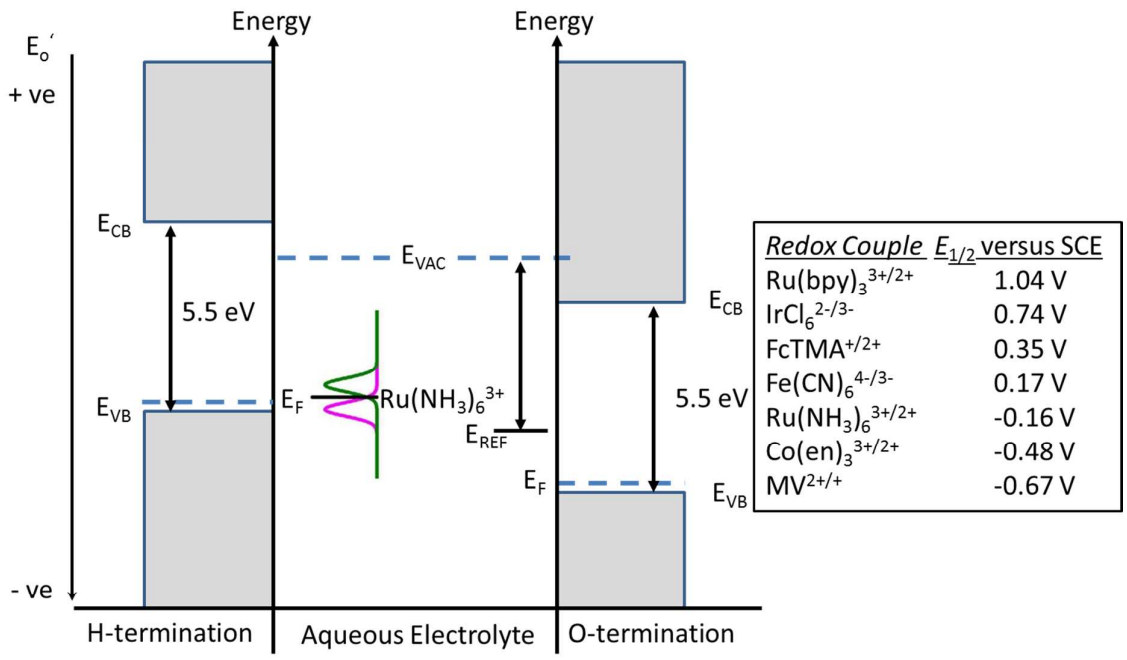

Figure 8: Schematic showing the approximate position of $Ru(NH_3)_6^{3+}$ with respect to E_{VB} and E_{CB} for both O- and H-terminated semiconducting BDD. $E_{1/2}$ values for different outer sphere redox mediators and $Fe(CN)_6^{4-/3-}$ taken from references 19 and [86].

Under these conditions, reversible CVs should only be recorded for electrodes where metallic conduction is the dominant electrical transport mechanism,[19,87,88] as with conventional metal electrodes such as Pt, Au *etc*. A reversible CV is one that is limited only by diffusion of redox species, as the ET rate constant, k_r, is much faster than the diffusional rate constant, k_t. For example, for an macrodisc electrode scanned at a potential scan rate, ν, in a quiescent solution containing excess supporting electrolyte k_t is given by:

$$k_t = \frac{2.69\text{x}10^5 n^{1/2} D^{1/2} c}{F} \qquad (3)$$

Assuming $n = 1$, $\nu = 0.1$ V s^{-1} and $D = 1 \times 10^{-5}$ cm^2 s^{-1}, $k_t = 0.0028$ cm s^{-1}. Hence to attain reversibility, with the electrode supplying sufficient charge carriers to maintain a potential-dependant Nernstian equilibrium, $k_r > k_t$.

This concept is illustrated in Figure 9(a) for differently doped BDD electrodes with the redox couple $Ru(NH_3)_6^{3+/2+}$ which we have employed to identify **non**-degenerately doped BDD. Furthermore, the outer sphere nature of the redox couple means that the response will depend only on the number of available charge carriers at a defined potential and interactions between the redox molecule and the surface need not be considered. Other redox species could be used if they fit these criteria, as shown in Figure 8. The choice of O-termination over H-termination for this measurement is also discussed below.

Note Figure 8 is an approximate guide. It can be difficult to accurately assign the known energy levels of the redox species to the band diagram of polycrystalline semi-conducting BDD, as the material characteristics of the BDD are typically inhomogeneous e.g. defect density, impurity and NDC content, boron dopant density, surface polarity (chemical functionality) and all play a role in precisely defining the energy level diagram. Moreover, impurities and defects can also contribute energy states in the band gap.[25] Polycrystalline BDD is not a perfect semiconductor. These are likely explanations for why: (i) a wide range of E_{FB} values have been reported for both semi-conducting O- and H-terminated BDD electrodes, for example as described in references [25, 89, 90] and (ii) redox species which are proposed to lie in the band gap of semi-conducting BDD can show a non-zero "kinetically limited" CV response.[25,19] It is thus useful to investigate the electrochemical response of the O-terminated BDD electrode towards a wide a range of outer sphere redox mediators, with different E_o' values, to help verify the metal-like status of the BDD.

The redox species of choice for characterising any newly prepared electrode used to be $Fe(CN)_6^{4-/3-}$. However, many papers over a significant time period have shown that this couple appears surface sensitive and electrolysis can lead to potential fouling of the electrode.[91, 92,86] On BDD, the $Fe(CN)_6^{4-/3-}$ couple is also one of the most studied redox systems but the results are variable,[26,51,44,19, 87, 93,94] with a wide range of ET kinetic rate

constants, k_o, recorded due to the apparent sensitivity of $Fe(CN)_6^{4-/3-}$ to surface functional groups, NDC content *etc*. Hence we advise using $Fe(CN)_6^{4-/3-}$ with caution when assessing the suitability of an unknown BDD electrode for electrochemical research.

CV Analysis: In a CV measurement, an indication of k_o can be obtained from measurement of the peak-to-peak separation, ΔE_p, for a range of different scan rates.[95] For accurate quantification the peaks should be at least 10 mV away from the position of reversibility,[96, 97] and both the resistance of the material (Figure 3) and non-faradaic current contributions should be accounted for. Material resistance is only likely to play a role *e.g.* in ohmic drop, if the currents passed are considerably high, due to high concentrations being employed. Note, EIS could also be employed to elucidate k_o from the measured charge transfer resistance.

If the diamond is doped degenerately a reversible (or close to reversible) faradaic peak current (i_p) response should be recorded for fast ET transfer outer sphere redox couples, over a wide E_o' range at a BDD macroelectrode in stationary solution. i_p can be predicted using the Randles Sevcik equation, equation 3, assuming linear diffusion dominates.[95]

$$i_p = 2.69\text{x}10^5 n^{3/2} A D^{1/2} v^{1/2} c \qquad (4)$$

c is the concentration of the species of interest. Additionally ΔE_p should be (or close to, within 10 mV[96, 97]) 59 mV / n (assuming a temperature of 25 ^oC).[95]

Figure 9(a) shows reversible CV behaviour for $Ru(NH_3)_6^{3+/2+}$ electrolysis at MC BDD electrodes doped with 1.9×10^{20} (purple) and 3×10^{20} (green) B atoms cm^{-3}. If the diamond is doped below the metallic threshold, as the BDD becomes depleted of charge carriers in the potential region of interest, electrolysis of $Ru(NH_3)_6^{3+/2+}$ (Figure 8) results in **non-reversible** CVs, also shown in Figure 9(a) (for dopant densities of mid 10^{19}'s, blue; 2×10^{18} red; and 9.2×10^{16} black, respectively). This effect is exacerbated as the boron dopant density decreases.[19]

Note significant NDC presence in the matrix can affect the CV response, as it may provide "conducting" sites for turnover of the redox mediator i.e. a semi-conducting electrode may appear conducting, or conversely may reduce the number of free charge carriers available.[98] Hence, it is essential NDC presence is taken into account when evaluating the electrochemical performance of the electrode with this redox couple. This is even more important when interpretating the response of inner sphere redox couples, where surface interactions are important.[54]

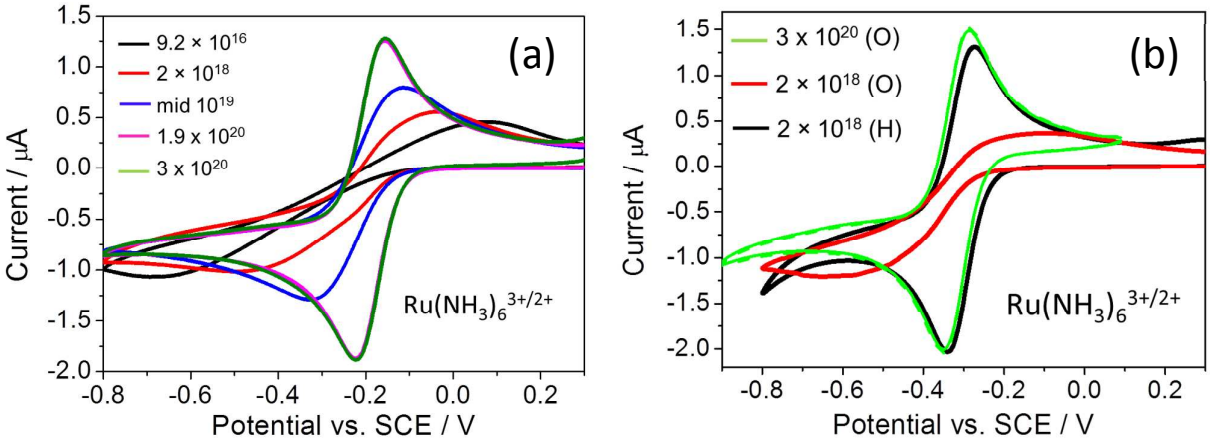

Figure 9: (a) CVs performed with a 1 mm diameter disc polished MC BDD electrode of dopant density 9.2 × 10^{16} (black line), 2 × 10^{18} (red line), mid 10^{19} (blue line), 1.9 × 10^{20} (pink line) and 3.2 × 10^{20} (green line) at a scan rate of 0.1 V s^{-1} for the reduction of 1 mM $Ru(NH_3)_6^{3+}$ in 0.1 M KNO_3. Taken from reference [19] with permission.(b) CVs recorded on a H-terminated (black line) and O-terminated (red line) MC BDD semi-conducting electrode (2 × 10^{18}). Comparison is made with an O-terminated "metallic" MC BDD electrode (3.2 × 10^{20} green line). Taken from reference [19] with permission.

For electrochemical measurements the additional surface conductivity H-termination imparts and the resulting movement in E_{CB} and E_{VB} (Figure 8) typically impacts negligibly for fast ET outer sphere redox couples on highly doped "metal-like" electrodes. This is due to the high number of already available charge carriers. Hence the CVs for "metal-like" O- and H-terminated BDD have been shown to appear reversible for $Ru(NH_3)_6^{3+/2+}$ electrolysis.[19] However, this is not true of semi-conducting electrodes. For the same 2 × 10^{18} B atoms cm^{-3}

electrode, ΔE_p for $Ru(NH)_6^{3+/2+}$ is much larger *i.e.* slower ET kinetics, for the O-terminated surface compared to its H-terminated counterpart, Figure 9(b). Note, the equations used to determine k_o, from CV analysis, for a semi-conducting electrode are different to those for a "metallic" one.[19,99] Dependant on the dopant density and redox couple, E_o', a H-terminated semi-conducting electrode may even look electrochemically reversible, which could result in misleading information about the dopant density of the electrode unless correctly accounted for. As the H-termination will not last forever, H-terminating a semi-conducting surface to improve its ET capabilities is not a viable approach long term.

Highly doped BDD, above the metallic threshold, can be thought of a metal with a lower DOS, compared to conventional metals such as Pt, Au. Metals typically have a DOS of ~10^{23} cm^{-3} eV^{-1}. For polished, MC BDD of average boron dopant density 5×10^{20} B atoms cm^{-3}, high resolution scanning electrochemical cell microscopy which can target individual grains and measure the local capacitance, determined the DOS, at 0.0 V versus Ag|AgCl, as varying between ~ 2×10^{20} cm^{-3} eV^{-1} and ~ 6×10^{20} cm^{-3} eV^{-1} *i.e.* at least two orders of magnitude smaller than a metal.[27] As the DOS effects the ET properties, which also relates to the number of available charge carriers and their mobility, ET rates for $Ru(NH_3)_6^{3+}$ and $FcTMA^+$ were elucidated and found to be ~ two orders of magnitude smaller than that for a classical metal.[27] However, the ET rates are still fast enough that when using BDD macro-sized electrodes with conventional CV techniques in quiescent solutions, diffusion is rate limiting for these outer sphere couples and the CV will look reversible, as shown in Figure 9(a).

Summary of recommendations

In order to enable useful comparisons between data in the literature and understand the results of your electrochemical measurement, it is important to understand the material attributes of your diamond electrode in parallel. The key parameters are:

(i) Boron concentration, the electrode should contain boron at levels > 10^{20} B atoms cm^{-3} to be considered metallic. This value can be obtained quantitatively from SIMS and qualitatively from Raman, where a Fano resonance will be observed in the diamond sp^3 peak, for "metallic" diamond. Electrical measurements, made under variable temperature conditions, will reveal the electrical transport mechanism which is intimately linked to boron concentration.

(ii) Surface morphology and grain size. Is the diamond MC, NC or UNC? This becomes important when considering NDC presence, calculating C_{dl}, modifying the surface and assessing the impact of potential heterogeneities associated with differently doped grains.

(iii) NDC content, this can be qualitatively assessed using Raman (but it is important to state the laser wavelength employed) and identified in electrochemical solvent window CVs, where an ORR signal is apparent and/or an oxidative currents due to surface NDC driven electrochemical redox processes.

(iv) Solvent window magnitude and capacitance, quoting also electrolyte / pH conditions, surface termination and the current magnitude employed to define the solvent window, to enable comparison with other groups.

(v) The surface termination (chemistry), most accurately recorded using XPS, but qualitatively indicated by contact angle. The latter is especially useful as a guide to indicating whether the surface is O- or H-terminated. It is important to recognise that surface termination effects the band energy positions and may also change with use, and is an important consideration when interpretating inner sphere ET. Note a H-terminated surface

may make a semi-conducting BDD electrode appear "metal-like" dependant on the E_o' of the redox couple of interest.

(vi) The response of the electrode towards outer sphere fast ET couples, which have an E_o' lying in the band gap of O-terminated semi-conducting BDD *e.g.* Ru $(NH_3)_6^{3+/2+}$. If the diamond is sufficiently doped to be metallic, under conditions where $k_r > k_t$, a CV recorded in quiescent solution (e.g. 1 mM concentration) at e.g. 0.1 V s^{-1} at a macroelectrode (e.g. diameter ~ mm) should appear reversible.

All these different factors need to be taken into account when evaluating the electrochemical performance of the electrode towards the redox species of interest.

Conclusions

There are a multitude of papers in the literature on the use of diamond electrodes in electroanalysis and electrochemical research. As conducting diamond is not your typical classical metal electrode understanding how to grow this material and use it electrochemically has advanced over the years, with input from materials scientists, chemists and physicists, significantly aiding understanding and improving material quality. As growth conditions are essential in controlling the material properties of the diamond electrode produced, one diamond electrode can be very different to the next. Compared to other electrodes such as Pt, Au, GC, the variability in material characteristics is probably the greatest for the "diamond" class of electrode materials, with UNC, NC and MC polycrystalline BDD all falling into this category and each with differing material characteristics that vary not only between the different sub-sets but also within a sub-set.

This protocols article aims to provide a useful reference point for any researcher wishing to commence work with diamond electrodes, providing practical details on how to characterise the electrode material before use, in order to best interpret the results obtained.

Full knowledge of the material properties of the electrode will also be invaluable, when comparing data from different laboratories, which use different diamond electrodes, but are working on the same experimental systems.

Acknowledgements: JVM would like to thank Prof. Greg Swain (University of Michigan) Dr. Katherine Holt (University College London) and Prof. Mark Newton (University of Warwick) for providing helpful comments and the diamond researchers (past and present) in the Warwick Electrochemistry and Interfaces Group whose insightful questions and comments on BDD electrodes over the years have been instrumental in shaping this article.

Table 1: List of commercial companies selling BDD electrodes,

Diamond supplier	Material Properties
Advanced Diamond Technology http://www.thindiamond.com/	UNCD thin film BDD electrodes aimed at water treatment
CCL Diamond http://www.ccl-diamond.com/HTML/Products_Electrodes.html	MC thin film BDD electrodes Coated on Ti, W, Nb, Si
Condias (DIACHEM®) http://condias.de/en/products/diachem/index.html	MC thin film BDD electrodes Coated on Nb, Ta, Si, Graphite, conductive ceramics Thickness up to 15 µm
Element Six http://www.e6.com/wps/wcm/connect/E6_Content_EN/Home/Applications/sensors/	DIAFILM EA grade (electroanalysis) Microcrystalline freestanding ~ 500 µm thick Boron concentration ~ 3×10^{20} Resistivity 45 mΩ cm Diamond insulated co-planar BDD macrodisk electrodes DIAFILM EP grade (processing)
NeoCoat Electrodes http://www.neocoat.ch/en/products/electrodes/	MC thin film BDD electrode Coated on Nb, Ta or Si Boron concentration (3×10^{19} - 3×10^{21}) Thickness 2-5 µm Resistivity 2 - 500 mΩ cm Recessed MEA and interdigitated array electrodes also available

REFERENCES

1. A. J. Bard, *Journal of the American Chemical Society*, 2010, 132, 7559-7567.
2. R. L. McCreery, *Chemical Reviews*, 2008, 108, 2646-2687.
3. J. C. Angus, in *Synthetic Diamond Films*, John Wiley & Sons, Inc., 2011, DOI: 10.1002/9781118062364.ch1, pp. 1-19.
4. Y. Einaga, J. S. Foord and G. M. Swain, *Mrs Bulletin*, 2014, 39, 525-532.
5. J. H. T. Luong, K. B. Male and J. D. Glennon, *Analyst*, 2009, 134, 1965-1979.
6. Y. Einaga, *J Appl Electrochem*, 2010, 40, 1807-1816.
7. Y. V. Pleskov, in *Advances in Electrochemical Science and Engineering, Volume 8*, Wiley-VCH Verlag GmbH & Co. KGaA, 2003, DOI: 10.1002/3527600787.ch3, pp. 209-269.
8. C. A. M.-H. Enric Brillas, *Synthetic Diamond Films: Preparation, Electrochemistry, Characterization, and Applications*, John Wiley and Sons, 2011.
9. Y. E. A. Fujishima, T. R. Rao and D. A. Tryk *Diamond Electrochemistry*, Elsevier, 2005.
10. R. S. Balmer, J. R. Brandon, S. L. Clewes, H. K. Dhillon, J. M. Dodson, I. Friel, P. N. Inglis, T. D. Madgwick, M. L. Markham, T. P. Mollart, N. Perkins, G. A. Scarsbrook, D. J. Twitchen, A. J.

Whitehead, J. J. Wilman and S. M. Woollard, *Journal of Physics: Condensed Matter*, 2009, 21, 364221.
11. F. P. Bundy, H. T. Hall, H. M. Strong and R. H. Wentorf, *Nature*, 1955, 176, 51-55.
12. Y. S. a. M. Kamo, *Synthesis of Diamond from the Vapour Phase*, Academic Press, London, 1992.
13. S. Morooka, T. Fukui, K. Semoto, T. Tsubota, T. Saito, K. Kusakabe, H. Maeda, Y. Hayashi and T. Asano, *Diamond and Related Materials*, 1999, 8, 42-47.
14. J. E. Butler, Y. A. Mankelevich, A. Cheesman, J. Ma and M. N. R. Ashfold, *Journal of Physics: Condensed Matter*, 2009, 21, 364201.
15. O. A. Williams, *Diamond and Related Materials*, 2011, 20, 621-640.
16. P. W. May and Y. A. Mankelevich, *The Journal of Physical Chemistry C*, 2008, 112, 12432-12441.
17. N. R. Wilson, S. L. Clewes, M. E. Newton, P. R. Unwin and J. V. Macpherson, *The Journal of Physical Chemistry B*, 2006, 110, 5639-5646.
18. G. Janssen, W. J. P. van Enckevort, W. Vollenberg and L. J. Giling, *Diamond and Related Materials*, 1992, 1, 789-800.
19. L. A. Hutton, J. G. Iacobini, E. Bitziou, R. B. Channon, M. E. Newton and J. V. Macpherson, *Analytical Chemistry*, 2013, 85, 7230-7240.
20. F. P. Bundy, *The Journal of Chemical Physics*, 1963, 38, 631-643.
21. T. Teraji, S. Mitani, C. Wang and T. Ito, *Journal of Crystal Growth*, 2002, 235, 287-292.
22. J. Achard, F. Silva, R. Issaoui, O. Brinza, A. Tallaire, H. Schneider, K. Isoird, H. Ding, S. Koné, M. A. Pinault, F. Jomard and A. Gicquel, *Diamond and Related Materials*, 2011, 20, 145-152.
23. H. V. Patten, S. C. S. Lai, J. V. Macpherson and P. R. Unwin, *Analytical Chemistry*, 2012, 84, 5427-5432.
24. L. Hutton, M. E. Newton, P. R. Unwin and J. V. Macpherson, *Analytical Chemistry*, 2009, 81, 1023-1032.
25. M. C. Granger, M. Witek, J. Xu, J. Wang, M. Hupert, A. Hanks, M. D. Koppang, J. E. Butler, G. Lucazeau, M. Mermoux, J. W. Strojek and G. M. Swain, *Analytical Chemistry*, 2000, 72, 3793-3804.
26. I. Duo, C. Levy-Clement, A. Fujishima and C. Comninellis, *Journal of Applied Electrochemistry*, 2004, 34, 935-943.
27. H. V. Patten, K. E. Meadows, L. A. Hutton, J. G. Iacobini, D. Battistel, K. McKelvey, A. W. Colburn, M. E. Newton, J. V. Macpherson and P. R. Unwin, *Angewandte Chemie International Edition*, 2012, 51, 7002-7006.
28. S. Wang, V. M. Swope, J. E. Butler, T. Feygelson and G. M. Swain, *Diamond and Related Materials*, 2009, 18, 669-677.
29. X. Blase, E. Bustarret, C. Chapelier, T. Klein and C. Marcenat, *Nat Mater*, 2009, 8, 375-382.
30. J. P. Lagrange, A. Deneuville and E. Gheeraert, *Diamond and Related Materials*, 1998, 7, 1390-1393.
31. K. Gelderman, L. Lee and S. W. Donne, *Journal of Chemical Education*, 2007, 84, 685.
32. D.C.Giancoli, *Physics: Principles with Applications* Prentice Hall, 4th edn., 1995.
33. W. J. Albery, G. J. O'Shea and A. L. Smith, *Journal of the Chemical Society, Faraday Transactions*, 1996, 92, 4083-4085.
34. A. F. Azevedo, M. R. Baldan and N. G. Ferreira, *Journal of Physics and Chemistry of Solids*, 2013, 74, 599-604.
35. R. M. Chrenko, *Physical Review B*, 1973, 7, 4560-4567.
36. P. Muret, J. Pernot, A. Kumar, L. Magaud, C. Mer-Calfati and P. Bergonzo, *Physical Review B*, 2010, 81, 235205.
37. F. Maier, M. Riedel, B. Mantel, J. Ristein and L. Ley, *Physical Review Letters*, 2000, 85, 3472-3475.
38. J. Ristein, *Journal of Physics D: Applied Physics*, 2006, 39, R71.

39. J. Ristein, *Appl. Phys. A*, 2006, 82, 377-384.
40. H. Kawarada, *Surface Science Reports*, 1996, 26, 205-259.
41. R. Boukherroub, X. Wallart, S. Szunerits, B. Marcus, P. Bouvier and M. Mermoux, *Electrochemistry Communications*, 2005, 7, 937-940.
42. E. Vanhove, J. de Sanoit, J. C. Arnault, S. Saada, C. Mer, P. Mailley, P. Bergonzo and M. Nesladek, *physica status solidi (a)*, 2007, 204, 2931-2939.
43. G. R. Salazar-Banda, L. S. Andrade, P. A. P. Nascente, P. S. Pizani, R. C. Rocha-Filho and L. A. Avaca, *Electrochimica Acta*, 2006, 51, 4612-4619.
44. I. Yagi, H. Notsu, T. Kondo, D. A. Tryk and A. Fujishima, *Journal of Electroanalytical Chemistry*, 1999, 473, 173-178.
45. F. B. Liu, J. D. Wang, B. Liu, X. M. Li and D. R. Chen, *Diamond and Related Materials*, 2007, 16, 454-460.
46. H. Notsu, I. Yagi, T. Tatsuma, D. A. Tryk and A. Fujishima, *Journal of Electroanalytical Chemistry*, 2000, 492, 31-37.
47. L. Ostrovskaya, V. Perevertailo, V. Ralchenko, A. Dementjev and O. Loginova, *Diamond and Related Materials*, 2002, 11, 845-850.
48. H. A. Girard, N. Simon, D. Ballutaud, E. de La Rochefoucauld and A. Etcheberry, *Diamond and Related Materials*, 2007, 16, 888-891.
49. C. H. Goeting, F. Marken, A. Gutiérrez-Sosa, R. G. Compton and J. S. Foord, *Diamond and Related Materials*, 2000, 9, 390-396.
50. R. E. Thomas, R. A. Rudder and R. J. Markunas, *Journal of Vacuum Science & Technology a-Vacuum Surfaces and Films*, 1992, 10, 2451-2457.
51. M. C. Granger and G. M. Swain, *Journal of The Electrochemical Society*, 1999, 146, 4551-4558.
52. H. B. Suffredini, V. A. Pedrosa, L. Codognoto, S. A. S. Machado, R. C. Rocha-Filho and L. A. Avaca, *Electrochimica Acta*, 2004, 49, 4021-4026.
53. R. Hoffmann, A. Kriele, H. Obloh, J. Hees, M. Wolfer, W. Smirnov, N. Yang and C. E. Nebel, *Applied Physics Letters*, 2010, 97, -.
54. J. A. Bennett, J. Wang, Y. Show and G. M. Swain, *Journal of The Electrochemical Society*, 2004, 151, E306-E313.
55. A. N. Patel, S.-y. Tan, T. S. Miller, J. V. Macpherson and P. R. Unwin, *Analytical Chemistry*, 2013, 85, 11755-11764.
56. D. Medeiros de Araújo, P. Cañizares, C. A. Martínez-Huitle and M. A. Rodrigo, *Electrochemistry Communications*, 2014, 47, 37-40.
57. A. C. Ferrari and J. Robertson, *Physical Review B*, 2000, 61, 14095-14107.
58. Y. Show, M. A. Witek, P. Sonthalia and G. M. Swain, *Chemistry of Materials*, 2003, 15, 879-888.
59. C. Lévy-Clément, N. A. Ndao, A. Katty, M. Bernard, A. Deneuville, C. Comninellis and A. Fujishima, *Diamond and Related Materials*, 2003, 12, 606-612.
60. K. Ushizawa, K. Watanabe, T. Ando, I. Sakaguchi, M. Nishitani-Gamo, Y. Sato and H. Kanda, *Diamond and Related Materials*, 1998, 7, 1719-1722.
61. F. Pruvost and A. Deneuville, *Diamond and Related Materials*, 2001, 10, 531-535.
62. J. Filik, J. N. Harvey, N. L. Allan, P. W. May, J. E. P. Dahl, S. Liu and R. M. K. Carlson, *Physical Review B*, 2006, 74, 035423.
63. H. Kuzmany, R. Pfeiffer, N. Salk and B. Günther, *Carbon*, 2004, 42, 911-917.
64. A. C. Ferrari and J. Robertson, *Physical Review B*, 2001, 63, 121405.
65. S. R. Waldvogel, A. Kirste and S. Mentizi, in *Synthetic Diamond Films*, John Wiley & Sons, Inc., 2011, DOI: 10.1002/9781118062364.ch19, pp. 483-510.
66. M. Werner, *Semiconductor Science and Technology*, 2003, 18, S41.
67. K. Das, V. Venkatesan, K. Miyata, D. L. Dreifus and J. T. Glass, *Thin Solid Films*, 1992, 212, 19-24.

68. D. Doneddu, O. J. Guy, P. R. Dunstan, T. G. G. Maffeis, K. S. Teng, S. P. Wilks, P. Igic, D. Twitchen and R. M. Clement, *Surface Science*, 2008, 602, 1135-1140.
69. S. Jolley, M. Koppang, T. Jackson and G. M. Swain, *Analytical Chemistry*, 1997, 69, 4099-4107.
70. M. B. Joseph, E. Bitziou, T. L. Read, L. Meng, N. L. Palmer, T. P. Mollart, M. E. Newton and J. V. Macpherson, *Analytical Chemistry*, 2014, 86, 5238-5244.
71. W. Smirnov, N. Yang, R. Hoffmann, J. Hees, H. Obloh, W. Müller-Sebert and C. E. Nebel, *Analytical Chemistry*, 2011, 83, 7438-7443.
72. J. Hees, R. Hoffmann, A. Kriele, W. Smirnov, H. Obloh, K. Glorer, B. Raynor, R. Driad, N. Yang, O. A. Williams and C. E. Nebel, *ACS Nano*, 2011, 5, 3339-3346.
73. K. L. Soh, W. P. Kang, J. L. Davidson, Y. M. Wong, D. E. Cliffel and G. M. Swain, *Diamond and Related Materials*, 2008, 17, 240-246.
74. A. Suzuki, T. A. Ivandini, K. Yoshimi, A. Fujishima, G. Oyama, T. Nakazato, N. Hattori, S. Kitazawa and Y. Einaga, *Analytical Chemistry*, 2007, 79, 8608-8615.
75. K. B. Holt, J. Hu and J. S. Foord, *Analytical Chemistry*, 2007, 79, 2556-2561.
76. J. Cvačka, V. Quaiserová, J. Park, Y. Show, A. Muck and G. M. Swain, *Analytical Chemistry*, 2003, 75, 2678-2687.
77. A. E. Fischer, Y. Show and G. M. Swain, *Analytical Chemistry*, 2004, 76, 2553-2560.
78. D. A. Tryk, K. Tsunozaki, T. N. Rao and A. Fujishima, *Diamond and Related Materials*, 2001, 10, 1804-1809.
79. N. Ramaswamy and S. Mukerjee, *The Journal of Physical Chemistry C*, 2011, 115, 18015-18026.
80. A. N. Correia and S. A. S. Machado, *Electrochimica Acta*, 1998, 43, 367-373.
81. K. F. Blurton, *Electrochimica Acta*, 1973, 18, 869-875.
82. K. B. Holt, A. J. Bard, Y. Show and G. M. Swain, *The Journal of Physical Chemistry B*, 2004, 108, 15117-15127.
83. Z. V. Živcová, O. Frank, V. Petrák, H. Tarábková, J. Vacík, M. Nesládek and L. Kavan, *Electrochimica Acta*, 2013, 87, 518-525.
84. R.N.Adams, *Electrochemistry at Solid Electrodes*, Marcel Dekker, 1969.
85. J. C. Ho, M. L.; Cramer, C. J.; Truhlar, D. G., *Theoretical Calculation of Reduction Potentials. Organic Electrochemistry*, CRC Press, Boca Raton, FL,, 5th edn., 2013.
86. K. K. Cline, M. T. McDermott and R. L. McCreery, *The Journal of Physical Chemistry*, 1994, 98, 5314-5319.
87. F. Marken, C. A. Paddon and D. Asogan, *Electrochemistry Communications*, 2002, 4, 62-66.
88. N. Vinokur, B. Miller, Y. Avyigal and R. Kalish, *Journal of The Electrochemical Society*, 1996, 143, L238-L240.
89. T. N. Rao, D. A. Tryk, K. Hashimoto and A. Fujishima, *Journal of The Electrochemical Society*, 1999, 146, 680-684.
90. H. A. Girard, N. Simon, D. Ballutaud and A. Etcheberry, *Comptes Rendus Chimie*, 2008, 11, 1010-1015.
91. S. C. S. Lai, A. N. Patel, K. McKelvey and P. R. Unwin, *Angewandte Chemie International Edition*, 2012, 51, 5405-5408.
92. D. Becker and K. Jüttner, *New Diamond and Frontier Carbon Technology*, 2003, 13, 67-78.
93. J. P. McEvoy and J. S. Foord, *Electrochim. Acta*, 2005, 50, 2933-2941.
94. M. Wang, N. Simon, C. Decorse-Pascanut, M. Bouttemy, A. Etcheberry, M. Li, R. Boukherroub and S. Szunerits, *Electrochimica Acta*, 2009, 54, 5818-5824.
95. A. J. B. a. L. R. Faulkner, *Electrochemical Methods: Fundamentals and Applications, 2nd Edition*, John Wiley & Sons.
96. A. N. Simonov, G. P. Morris, E. A. Mashkina, B. Bethwaite, K. Gillow, R. E. Baker, D. J. Gavaghan and A. M. Bond, *Analytical Chemistry*, 2014, DOI: 10.1021/ac5019952.

97. A. M. Bond, E. A. Mashkina and A. N. Simonov, in *Developments in Electrochemistry*, John Wiley & Sons, Ltd, 2014, DOI: 10.1002/9781118694404.ch2, pp. 21-47.
98. M. R. Baldan, A. F. Azevedo, A. B. Couto and N. G. Ferreira, *Journal of Physics and Chemistry of Solids*, 2013, 74, 1830-1835.
99. B. R. Horrocks, M. V. Mirkin and A. J. Bard, *The Journal of Physical Chemistry*, 1994, 98, 9106-9114.